

## PREPARATION AND STRUCTURAL CHARACTERIZATION OF MoS<sub>2</sub> NANOPARTICLE COATED GRAPHENE OXIDE/MANGANESE OXIDE COMPOSITE FOR ENERGY STORAGE APPLICATION

R. JOTHIRAMALINGAM<sup>a,b,\*</sup>, H. A. AL-LOHEDAN<sup>a</sup>, D. M. AL-DHAYAN<sup>a</sup>,  
M. D. WASMIAH<sup>b</sup>

<sup>a</sup>Chemistry Department, College of Science, King Saud University, Riyadh 11451, Saudi Arabia. <sup>b</sup>Surfactant Research Chair, Department of chemistry, College of Science, King Saud University, Riyadh 11451, Saudi Arabia.

Nanoparticles of powder molybdenum sulphide (MoS<sub>2</sub>) are deposited on reduced graphene oxide-mesoporous manganese oxide nanocomposite which is represented as MoSGMn were prepared by feasible ultrasonic assisted deposition technique. The above prepared nanocomposite is further coated on Nickel foam substrate for direct application towards supercapacitor electrode fabrication. The detailed studies of thermal property and surface property such as thermal stability, surface structure and zeta potential measurements have been explained for all prepared nanocomposite samples. The thermal stability of as prepared sample stable upto 350 °C in oxygen atmosphere and negative zeta potential obtained for all prepared nanocomposite sample. The different amount of MoS<sub>2</sub> nanoparticle (10mg -100 mg range) was utilized to study the effect of molybdenum sulphide addition on major mesoporous manganese oxide matrix. Increased quantity of MoS<sub>2</sub> addition increase the electrochemical supercapacitance value of the nanocomposite coated nickel foam modified electrode.

(Received January 29, 2020; Accepted April 16, 2020)

**Keywords:** Mesoporous, Nanoparticle MoS<sub>2</sub>, Manganese oxide, Graphene oxide, Super capacitor

### 1. Introduction

Porous manganese oxide with different type of dopant incorporated nanostructured material is fabricated by both oxidation and reduction routes from higher valent potassium permanganate as well as by oxidizing low cost manganese (II) precursors [1-5]. Porous manganese oxide is multivalent oxidation state and hence the foreign metal cation with suitable ionic radius or graphene like carbon compounds could deposit for improved electro catalytic performance [6-7]. There is a growing demand for electrode materials development in the field of battery and super capacitor devices. Manganese oxide is one the low cost and green chemical compound for sustainable development [8-13]. The porous manganese oxide is an eco-friendly transition metal oxide and its low cost precursor attracts it to make in large scale synthesis for various catalytic and renewable energy applications [10-15]. The different kind of preparation strategy adopted to make porous to mesoporous manganese oxide and also fabricate the nanoparticle of manganese oxide [16-18]. The porous chitosan-MnO<sub>2</sub> Nano hybrid like modified catalytic materials are utilized for a green and biodegradable heterogeneous catalyst for aerobic oxidation of alkylarenes and alcohols [19]. Co-precipitation method is adopted to synthesize the nanoparticles of gold and silver supported on porous manganese oxide were studied for catalytic properties of benzyl alcohol oxidation using molecular oxygen [20]. The catalytic results revealed that the catalyst calcined at higher optimized temperature (400 °C) is showing higher catalytic activity. Ceria (CeO<sub>2</sub>) modified manganese oxide is also play the important catalytic role in phenol removal and sorption capacity reaction, phenolic compounds are one of the model pollutant and also more toxic pollutant exist in the pharma and dye industry waste waters [21-22]. Thermal characterization of nanoparticle

---

\* Corresponding author: jrajabathar@ksu.edu.sa

modified porous manganese oxide catalysts are studied very rarely due to Meta stability nature of porous manganese oxide. After modification by thermally strong additive on porous manganese oxide is fabricated in the present study and studied their physico-chemical activity in details. In the present study is also aim to exploit the detailed characterization for surface structure of modified porous manganese oxide with the addition of graphene and MoS<sub>2</sub> nanoparticle deposition.

## 2. Materials and method

Manganese acetate, sodium hydroxide, non-ionic surfactant, molybdenum sulphide Nano powder and Nafion per fluorinated resin solution purchased from Sigma Aldrich. All chemicals are used in the present work were of analytical grades. Nickel foam with density of  $480 \pm 30 \text{ g/m}^2$  width and pore number =110 PPI, Thickness: 1.5. The Nickel foam substrate is used to coat the as prepared nanocomposite. X-ray diffraction (Miniflex 600), TEM images are recorded at acceleration voltage of 200 kV (JEOL-JEM-2100F, Japan). BET surface area analysis and Nitrogen adsorption desorption analysis studied (NOVA 2200e,USA). BRANSON Ultrasonicator (USA) with 20% amplitude of power is applied for all preparation.

### 2.1. Preparation of MoS<sub>2</sub>/graphene oxide/meso-MnO<sub>2</sub> nanocomposite

The starting material is mesoporous MnO<sub>2</sub> prepared by precipitation method using non-ionic surfactant, which is reported in our previous report elsewhere [21]. The nanocomposite fabrication carried out by two stage ultra-sonication method. Firstly the 0.5 g of graphene oxide is mixed with as prepared mesoporous manganese oxide in ethanol solution. The above mixed solution ultrasoinicated for 15 min with 20% of amplitude power under ultrasonic irradiation. In the second state appropriate amount of (100-50 mg) MoS<sub>2</sub> Nano powder was mixed with above prepared suspension of reduced graphene/meso-MnO<sub>2</sub> mixture to make the nanocomposite. The above prepared nanocomposite designated as MoSGMn-1 (100 mg of MoS<sub>2</sub>) and MoSGMn-2 (50 mg of MoS<sub>2</sub>).

### 2.3. Electrochemical activity and supercapacitor characterization

The nanocomposite coating is carried out on the one end of Nickel foam by strong pressing method. The area of loading the active materials is  $1 \text{ cm}^2$  (1cm x 1cm) in the required length of working electrode. The working electrodes were prepared by mixing MoSGMN-nanocomposite (95 wt.%) and 5 wt.% nafion to form a paste and drying at 80 °C in an oven for two hours. The mass of the electrode material was found to be approximately 5 mg. The electrolyte was a mixture of 1M H<sub>2</sub>SO<sub>4</sub> for better supporting electrolytic condition. Nafion (perfluorinated resin) solution used for working electrode preparation was obtained from Sigma–Aldrich. Nickel foam is used as binder free substrate in the present work, which is obtained from Winfay Group Company Limited, Shanghai, China.

## 3. Results and discussion

Powder X-ray diffraction pattern of as prepared samples are shown in Fig. 1. The major intense peaks are indexed and referred with standard reported XRD pattern of mesoporous manganese oxides. Fig. 1 shows the X-ray diffraction spectra of different amount of molybdenum sulphide nanoparticles deposited GO-MnO<sub>2</sub> nanocomposite. The crystalline phase of final composite consist of mesoporous Mn<sub>2</sub>O<sub>3</sub> phase as the major compound and the *hkl* plane values and *d*-space values of the synthesized nanocomposite are matched very well with reported mesoporous Mn<sub>2</sub>O<sub>3</sub> phase.

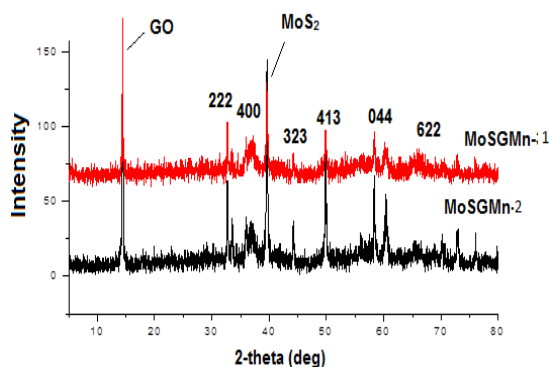


Figure. 1. XRD pattern of MoSGMn-1 (100 mg MoS<sub>2</sub>) and MoSGMn-2 (50 mg MoS<sub>2</sub>).

The FT-IR spectra of different amount of molybdenum sulphide deposited porous manganese oxide composite are shown in Fig. 2a and 2b. The Mn-O stretching frequency of MoSGMn-1 (100 mg of MoS<sub>2</sub>) is obtained at 573 cm<sup>-1</sup> and 744 cm<sup>-1</sup>. The other samples are also shown in the same region with slight alteration obtained, MoSGMn-2 (50 mg of MoS<sub>2</sub>) shows 566 and 741 cm<sup>-1</sup>. Hence addition of higher amount of MoS<sub>2</sub> into manganese oxide could effectively penetrate the oxide matrix for possible improvement or feasibility in the ionic transport process upon electrochemical reactions. The other chemical elements in the composite are Mo-S-Mo, C-C, C-O of reduced graphene oxide are also showing mixed stretching frequency of the respective chemical components present in the composite. In the case MoS<sub>2</sub>, the S-Mo-S stretching frequency usually occurred in the range of 1600-1700 cm<sup>-1</sup> [23,24]. The two new peaks are observed at 622 cm<sup>-1</sup> and 508 cm<sup>-1</sup> corresponding to the vibration of the Mn-O stretching modes, associated with Mn in tetrahedral and octahedral sites, respectively [25].

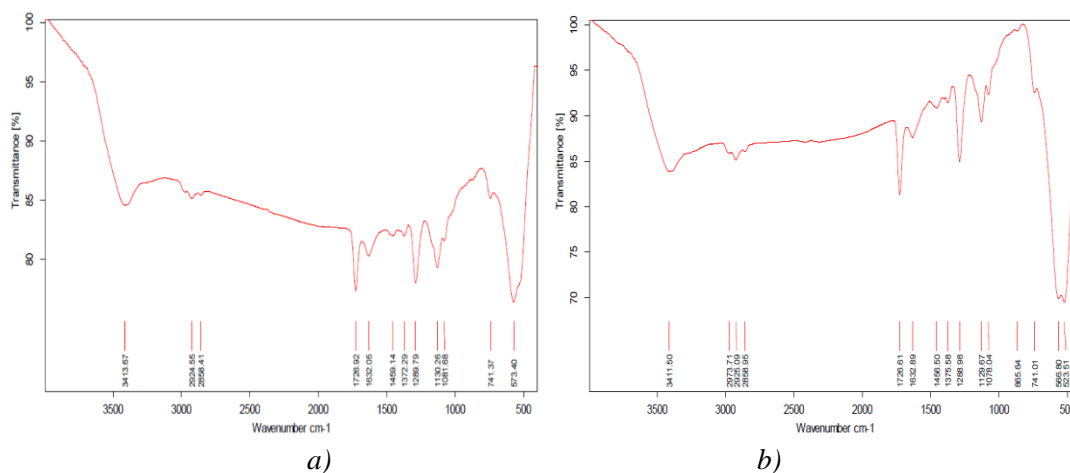


Figure (2a) FT-IR spectra of MoSGMn-1 and (2b) MoSGMn-2

Figure 3a and 3b shows the MoSGMn-1 and the dark and dense particles are due to strongly binded manganese oxide particle dispersion on flaky sheet morphology of reduced graphene oxide. The MoS<sub>2</sub> particles form dense needles aggregated with manganese oxide particles instead of very thin needle shape with lengthier nanotube for MoSGMn-2 (Fig 3c and 3d). The decreased amount of MoS<sub>2</sub> addition causes more transparent nanosheet morphology for as prepared mesoporous manganese oxide with flaky glassy graphene dispersion. The flaky sheet structure of reduced graphene oxide is finely intercalated with mesoporous manganese oxide and forms the dense composite structure. The Fig. (3c and 3d) shows the MoSGMn-2(50 mg) of MoS<sub>2</sub> addition on reduced graphene oxide-manganese oxide composite, in the case of less amount of

MoS<sub>2</sub> nanoparticle addition results leads in the formation of smooth dispersion of r-GO-dispersion. mesoporous manganese oxide (Fig. 3e). Fig. 3f shows the existence of all three initially added component aggregated together in the form fine needle shape (molybdenum sulphide) with dark spherical particles of manganese oxide and finely dispersed on

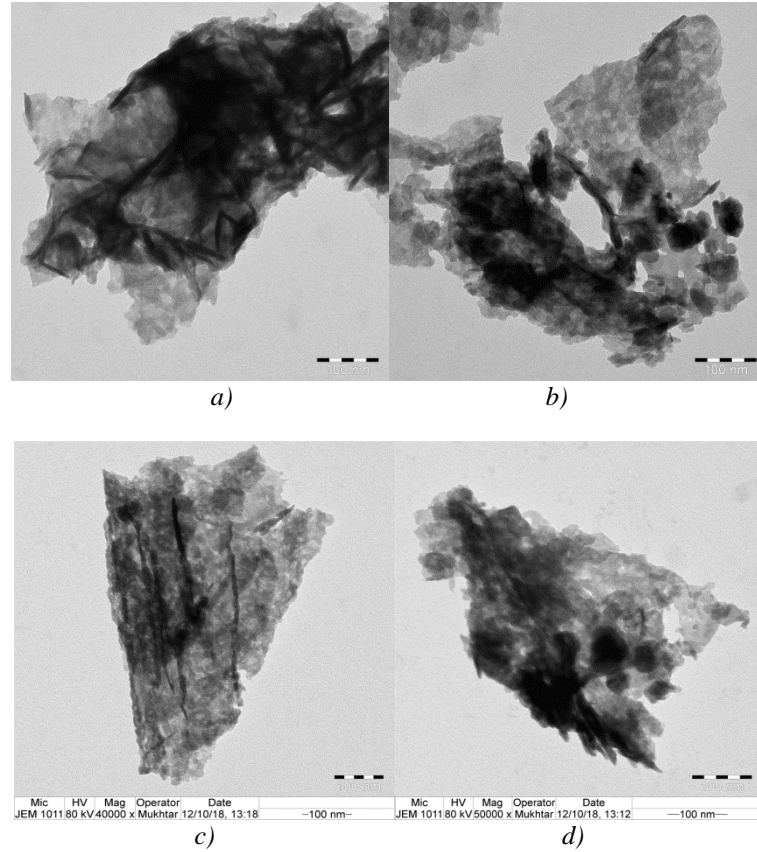


Figure 3 a), b) TEM image of MoSGMn-1;  
c), d) TEM image of MoSGMn -2

Fig. 3d shows the nanotubular shape morphology, which is very visible at below 50 nm scale and also nanoparticle deposited on glassy graphene oxide on mesoporous MnO<sub>2</sub>.

The Cyclic voltammetry (CV) analysis is carried out on different amount of MoS<sub>2</sub>/r-graphene oxide modified mesoporous manganese oxide for exploits its potential electrochemical activity at different scan rates ranging from 1-500 mV/s in acid electrolyte medium (1M sulphuric acid) . Fig. 4a and 4b shows the CV curves and curves are shows leaf like structure without any redox peaks indicating that the electrode material possess good electrical double-layer capacitance. The specific capacitance of the electrode materials is calculated by adopting below equation

$$C_{sp} = \frac{1}{vm(V-V_0)} \int_{V_0}^V I(V)dV \quad (1) [31]$$

$C_{sp}$  is the specific capacitance (F/g),  $v$  is the potential scan rate (V/s),  $V-V_0$  is the potential window (V),  $I$  is a current response in accordance with the sweep voltage (A) and  $m$  is the mass of the electrode. The specific capacitance values are given in Table 1 for all prepared samples at at different scan rate. The higher specific capacitance is obtained for MoSGMn-1 of MoS<sub>2</sub> incorporated r-GO deposited meso-manganese oxide and its efficiency gradually decreases by decreasing the amount of MoS<sub>2</sub> addition from 100mg (MoSGMn-1) to 50 mg (MoSGMn-2). The specific capacitance values are depends on the following factors: the needle and nanotube morphological MoS<sub>2</sub> deposition in manganese oxide could modify the ion diffusion process during

the charging/discharging process [26]. Secondly interconnected structure of the conducting graphene sheets will improve the electron transport phenomenon of the nanocomposite. The other possible factor is the presence and creation of new catalytic active site on porous matrix of major manganese oxide compound. Specific capacitance is decreased with increase in the scan rate for the as prepared nanocomposites. At low scan rates ions will get saturated time to transport into inner pores of the electrodes. Consequently large number of ions is adsorbed on the electrode surface are the main factor for improved capacitive behavior.

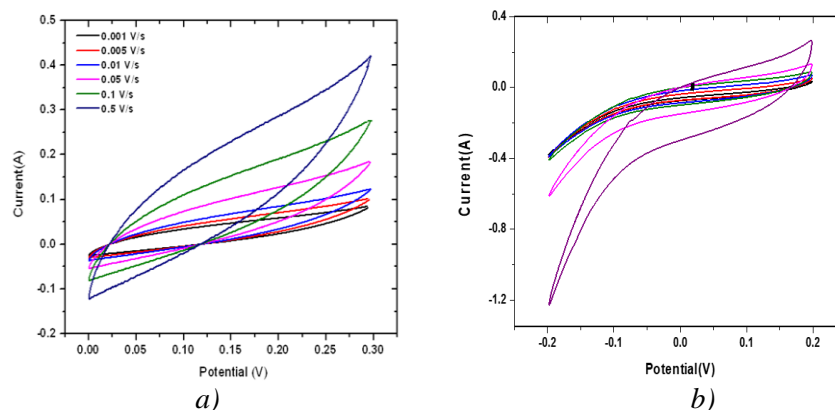


Figure 4 Cyclic voltammogramme curve of a)MoSGMn-1 and b)MoSGMn-2 at different scan rate in 1 M  $H_2SO_4$

Table 1. Specific capacitance (F/g) from CV studies at different scan rates.

can rate (V/s)	Specific Capacitance (F/g)	
Sample Code	MoSGMn-1	MoSGMn-2
0.001 V/s	527	1160
0.005 V/s	134	520
0.01V/s	76	208
0.05 V/s	27	91
0.1V/s	17	50
0.5 V/s	5	37

#### 4. Conclusion

The multicomponent nanocomposite based on  $MoS_2$  incorporated R-GO deposited mesoporous manganese oxide with  $Mn_2O_3$  phase nanomaterials was successfully developed by feasible two-step process for supercapacitor electrode fabrication. The Ft-IR spectra show the distinctive peaks for the presence of respective stretching frequency of manganese oxide, molybdenum sulphide and reduced graphene oxide in nanocomposite form. The highest specific capacitance obtained for MoSGMn-1 and MoSGMn-2 at 1mV/s is 1160 F/g and 527 F/g respectively. All these electrochemical parameters proofs that the prepared  $MoS_2$  nanoparticle modified r-GO/mesoMnO<sub>2</sub> on nickel foam electrode provide the promising supercapacitor device for renewable energy applications.

**Funding information:** The financial grant number – RSP2019/54

## Acknowledgements

The authors acknowledge the financial support through Researchers Supporting Project number (RSP 2019/54), King Saud University, Riyadh, Saudi Arabia.

## References

- [1] M. V. Reddy, G. V. Subba Rao, B. V. Chowdari, *Chem. Rev.* **113**, 5364 (2013).
- [2] H. L. Wang, Z. W. Xu, Z. Li, K. Cui, J. Ding, A. Kohandehghan, X. H. Tan, B. Zahir, B. C. Olsen, C. M. Holt, D. Mitlin, *Nano Lett.* **14**, 1987 (2014).
- [3] R. Jothi Ramalingam, Arun K. Shukla, Ali Aldalbahi, Hamad A. Al-Lohedan, *International Journal of Hydrogen Energy* 42(2017)15679-15688.
- [4] M. B. Sassin, A. N. Mansour, K. A. Pettigrew, D. R. Rolison, J. W. Long, *ACS Nano* **4**, 4505 (2010).
- [5] X. F. Zheng, H. E. Wang, C. Wang, Z. Deng, L. H. Chen, Y. Li, T. Hasan, B. L. Su, *Nano Energy* **22**, 269 (2016).
- [6] J. Jin, L. Wu, S. Z. Huang, M. Yan, H. E. Wang, L. H. Chen, T. Hasan, Y. Li, B. L. Su, *Small Methods* **2**, 1800171 (2018).
- [7] B. Long, L. Luo, J. Zhang, M. S. Balogun, S. Song, Y. Tong, *Mater. Today Energy* **9**, 311 (2018).
- [8] W. Zhang, J.Z. Sheng, J. Zhang, T. He, L. Hu, R. Wang, L. Q. Mai, S. C. Mu, *J. Mater. Chem. A* **4**, 16936 (2016).
- [9] R. Jothi Ramalingam, Mansoor-Ali Vaali-Mohammed, Hamad A. Al-Lohedan, Jimmy Nelson Appaturi, *Journal of Molecular Liquids*, 243 (2017) 348–357.
- [10] S. B. Wang, C. L. Xiao, Y. L. Xing, H. Z. Xu, S. C. Zhang, *J. Mater. Chem. A* **3**, 15591 (2015).
- [11] S. Z. Huang, Q. Zhang, W. B. Yu, X. Y. Yang, C. Wang, Y. Li, B. L. Su, *Electrochim. Acta* **222**, 561 (2016).
- [12] S. B. Wang, Y. B. Ren, G. R. Liu, Y. L. Xing, S. C. Zhang, *Nanoscale* **6**, 3508 (2014).
- [13] K. Y. Li, F. F. Shua, X. W. Guo, D. F. Xue, *Electrochim. Acta* **188**, 793 (2016).
- [14] D. Sun, Y. G. Tang, D. L. Ye, J. Yan, H. S. Zhou, H. Y. Wang, *ACS Appl Mater. Interf.* **9**, 5254 (2017).
- [15] J. Wang, C. B. Zhang, D. D. Jin, K. Y. Xie, B. Q. Wei, *J. Mater. Chem. A* **3**, 13699 (2015).
- [16] D. S. Liu, D. H. Liu, B. H. Hou, Y. Y. Wang, J. Z. Guo, Q. L. Ning, X. L. Wu, *Electrochim. Acta* **264**, 292 (2018).
- [17] J. Y. Wang, Q. L. Deng, M. J. Li, K. Jiang, Z. G. Hu, J. H. Chu, *Nanoscale* **10**, 2944 (2018).
- [18] T. Chen, Z. G. Wu, W. Xiang, E. H. Wang, T. R. Chen, X. D. Guo, Y. X. Chen, B. H. Zhong, *Electrochim. Acta* **246**, 931 (2017).
- [19] A. Shaabani, M. B. Boroujeni, M. S. Laeini, *Appl Organomet Chem.* **30**, 154 (2016).
- [20] M. Abecassis-Wolfovich, R. Jothiramalingam, M.V. Landau, M. Herskowitz, B. Viswanathan, T.K. Varadarajan, *Appl. Catal. B Environ.* 59 (2005) 91–98.
- [21] R. Jothi Ramalingam, Judith J. Vijaya, Arunachalam Prabakaran, Zuheir A. Issa, Ayman M. Atta, A.O. Ezzat, Abdullah M. Al-Mayouf, Hamad A. Al-Lohedan, *Journal of Alloys and Compounds* 698 (2017) 1077-1085
- [22] R. Jothi Ramalingam, Niketha Konikkara, Hamad Al-Lohedan, Dhaifallah M. Al-Dhayan, L. John Kennedy, S.K. Khadheer Basha, Shaban R.M. Sayed, *International Journal Of Hydrogen Energy* 43(2018)17121-17131.
- [23] R. Taziwa, E. L. Meyer, E. Sideras-Haddad, R. M. Erasmus, E. Manikandan, B. W. Mwakikunga, *Int. J. Photoenergy*, 1 (2012).